Interconversion of two oxidized forms of taurine/α-ketoglutarate dioxygenase, a non-heme iron hydroxylase: Evidence for bicarbonate binding

Matthew J. Ryle*, Kevin D. Koehntop†, Aimin Liu†‡, Lawrence Que, Jr.†, and Robert P. Hausinger*§

*Departments of Microbiology and Molecular Genetics and of Biochemistry and Molecular Biology, Michigan State University, East Lansing, MI 48824-4320; and †Center for Metals in Biocatalysis and Department of Chemistry, University of Minnesota, Minneapolis, MN 55455

Edited by JoAnne Stubbe, Massachusetts Institute of Technology, Cambridge, MA, and approved January 31, 2003 (received for review November 5, 2002)

Taurine/α-ketoglutarate (αKG) dioxygenase, or TauD, is a mononuclear non-heme iron hydroxylase that couples the oxidative decarboxylation of αKG to the decomposition of taurine, forming sulfite and aminoacetaldehyde. Prior studies revealed that taurine-free TauD catalyzes an O_2- and αKG-dependent self-hydroxylation reaction involving Tyr-73, yielding an Fe(III)-catecholate chromophore with a λ_{max} of 550 nm. Here, a chromophore (λ_{max} 720 nm) is described and shown to arise from O_2-dependent self-hydroxylation of TauD in the *absence* of αKG, but requiring the product succinate. A similar chromophore rapidly develops with the alternative oxidant H_2O_2. Resonance Raman spectra indicate that the ≈700-nm chromophore also arises from an Fe(III)-catecholate species, and site-directed mutagenesis studies again demonstrate Tyr-73 involvement. The ≈700-nm and 550-nm species are shown to interconvert by the addition or removal of bicarbonate, consistent with the αKG-derived CO_2 remaining tightly bound to the oxidized metal site as bicarbonate. The relevance of the metal-bound bicarbonate in TauD to reactions of other members of this enzyme family is discussed.

Taurine/α-ketoglutarate (αKG) dioxygenase, or TauD, catalyzes the conversion of taurine (2-aminoethanesulfonic acid) to sulfite and aminoacetaldehyde in the presence of O_2, αKG, and Fe(II) as shown in Scheme 1 (1). This *Escherichia coli* protein is a member of a rapidly expanding enzyme superfamily that utilizes mononuclear Fe(II) active sites to catalyze a diverse range of chemical transformations, usually coupled to the oxidative decarboxylation of an α-keto acid (2–4). Other family members include enzymes that modify protein side chains (5, 6), repair alkylation-damaged DNA (7), degrade compounds in the environment (8–11), and synthesize antibiotics (12–14), plant metabolites (15, 16), or other small molecules (17, 18). Most representatives carry out specific hydroxylation reactions, but examples of enzymes catalyzing desaturations, ring closures, and ring expansion reactions have also been documented (19). Regardless of their overall chemistry, these enzymes generally are thought to form a high-valent iron-oxo intermediate; however, such an intermediate has never been directly observed.

Recent studies of TauD and the herbicide-degrading enzyme TfdA, which share ≈30% sequence identity, have provided important insights into the reactivity of this group of enzymes (e.g., refs. 20–28). In the absence of substrates, Fe(II) is coordinated by three amino acid side chains in a two-His-one-carboxylate motif [His-99, Asp-101, and His-255 in TauD; and His-114, Asp-116, and His-262 in TfdA (23, 26)] and three water molecules to afford a six-coordinate metal center. αKG chelates to the Fe(II) and displaces two water molecules, binding through the 1-carboxylate and 2-keto moieties. The primary substrate binds near, but not directly to, the Fe(II), promoting loss of the final water ligand to yield a five-coordinate metal center (26), as illustrated in Fig. 1. The site vacated by water is thought to be the site of oxygen

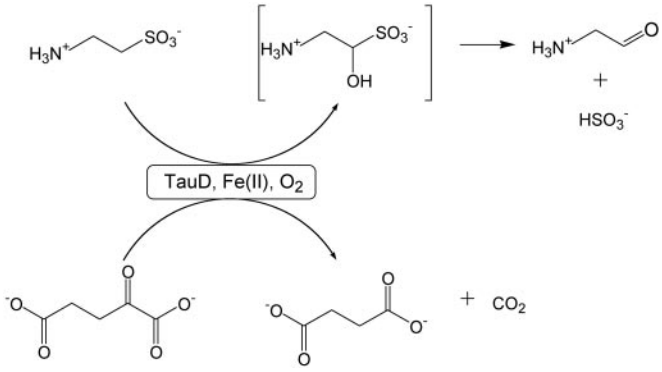

Scheme 1.

interaction, with subsequent catalytic steps remaining poorly defined.

In the absence of primary substrate, slow O_2-dependent self-hydroxylation reactions occur for both enzymes in a process requiring αKG decomposition. For example, αKG-Fe(II)TfdA reacts with oxygen to hydroxylate a tryptophan residue adjacent to a metal ligand (25). The resulting hydroxytryptophan coordinates the oxidized metal ion to yield a blue chromophore (λ_{max} 580 nm, ε_{580} 1,000 $M^{-1}\cdot cm^{-1}$). Oxygen exposure of αKG-Fe(II)TauD yields instead a greenish-brown chromophore (λ_{max} 550 nm, ε_{550} 700 $M^{-1}\cdot cm^{-1}$) arising from a catecholate ligand derived from the hydroxylation of Tyr-73 (28). In this latter reaction, evidence for the involvement of a transient tyrosyl radical (λ_{max} 408 nm, minimum ε_{408} 1,600 $M^{-1}\cdot cm^{-1}$) has been obtained. Self-hydroxylation reactions and uncoupled reactions that cause metal oxidation likely account for the autoinactivation behavior of these enzymes (e.g., 20, 27, 28). Analogous self-hydroxylation reactivity has also been reported for a synthetic analog that mimics features of αKG-dependent dioxygenases (29) and for other non-heme iron enzymes that activate oxygen. The latter include selected mutants of the R2 subunit of ribonucleotide reductase in which Phe or Tyr residues are hydroxylated (30, 31) and probably 4-hydroxyphenylpyruvate dioxygenase, whose blue color (λ_{max} 595 nm, ε_{595} 2,600 $M^{-1}\cdot cm^{-1}$) in the oxidized form arises from a Tyr residue (32) despite the absence of such residues at the active site (33). Thus, the oxygen

This paper was submitted directly (Track II) to the PNAS office.

Abbreviations: αKG, α-ketoglutarate; TauD, taurine/α-ketoglutarate dioxygenase; DAOCS, deacetoxycephalosporin C synthase; ACC, 1-aminocyclopropane-1-carboxylate.

‡Present address: Department of Biochemistry, University of Mississippi Medical Center, Jackson, MS 39216.

§To whom correspondence should be addressed: 6193 Biomedical and Physical Sciences, Department of Microbiology and Molecular Genetics, Michigan State University, East Lansing, MI 48824-4320. E-mail: hausinge@msu.edu.

www.pnas.org/cgi/doi/10.1073/pnas.0636740100

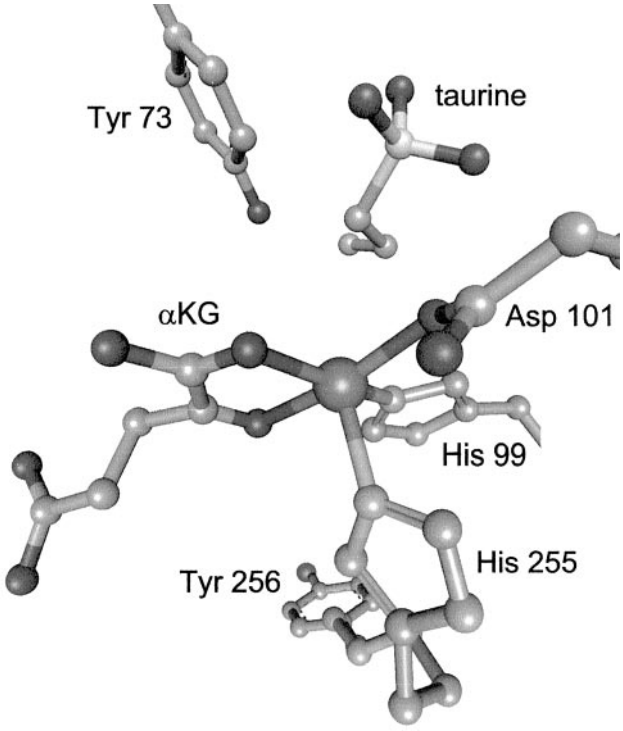

Fig. 1. TauD active site. The crystal structure of taurine-αKG-Fe(II)TauD (26) reveals that the metal ion is coordinated by His-99, Asp-101, and His-255 of the protein. The binding positions of the cosubstrates are shown with taurine near, but not coordinated to, the metal ion and αKG bound as a chelate. The positions of two Tyr residues located <10 Å from the metal ion also are shown.

reactivity of TauD and TfdA in the absence of their primary substrates may serve as a paradigm for understanding the self-hydroxylation chemistry found in the non-heme iron enzymes.

Here we report the generation of a chromophore with an absorption maximum near 720 nm arising from oxygen-dependent self-hydroxylation of TauD in the *absence* of αKG, but requiring the product, succinate. A very similar chromophore rapidly develops on treatment of succinate-Fe(II)TauD with the alternative oxidant hydrogen peroxide. Resonance Raman spectroscopy reveals that the ≈700-nm chromophore arises from catecholate-bound Fe(III) with a spectrum that is slightly perturbed from that associated with the 550-nm Fe(III)-catecholate chromophore. Site-directed mutagenesis studies demonstrate that the same tyrosine residue is modified in samples containing either the 550-nm or ≈700-nm chromophore. The two catecholate-based spectroscopic species are interconverted by the addition or removal of metal-bound bicarbonate. We discuss the relevance of these findings to reactions catalyzed by this enzyme family.

Methods

Purification of TauD. Ten-liter cultures of *E. coli* BL21(DE3)-(pME4141) cells expressing *tauD* were grown and harvested as previously described (1). TauD was purified as reported (21), except that phenylmethylsulfonylfluoride, leupeptin, and glycerol were excluded from the purification procedure. Purified enzyme was extensively dialyzed against 25 mM Tris buffer (pH 8.0) at 4°C and stored as frozen aliquots at −20°C. TauD activity was measured by using Ellman's reagent as described (1). Protein concentrations were determined by using a commercial protein assay (Bio-Rad) with standard curves prepared with preweighed BSA purchased from the same source. The TauD used in these studies exhibited k_{cat} values ranging from 2.6 to 4.2 s^{-1} based on a 1 μg/ml, 5-min assay. TauD variants were purified as described (28).

UV/Visible Spectroscopy of O_2- and H_2O_2-Treated Fe(II)TauD Samples. Reagent stock solutions of αKG, taurine, and succinate (30 mM) for UV/visible spectroscopic studies were prepared in 25 mM Tris buffer (pH 8.0) inside serum vials sealed with butyl rubber stoppers. The solutions were made anaerobic by several rounds of vacuum degassing and flushing with argon by using a vacuum manifold. Ferrous ammonium sulfate stock solutions (30 mM) were prepared inside a sealed serum vial by adding anaerobic water and flushing with several rounds of argon. UV/visible spectroscopic studies used a 1-cm path length, 2-ml quartz cuvette fitted with a stopper and purged of oxygen by flushing with argon. Anaerobic TauD was transferred into the cuvette by using a gas-tight syringe (Hamilton) that had been flushed with anaerobic buffer, and other reagents were added. The samples were oxidized by filling the headspace with oxygen, mixing with an equal volume of O_2-saturated buffer, or titrating with H_2O_2, and spectra were recorded as indicated.

Raman Spectroscopy. Resonance Raman spectra were collected on an Acton (Acton, MA) AM-506 spectrometer (1,200-groove grating) by using a Kaiser Optical Systems (Ann Arbor, MI) holographic supernotch filter and a Princeton Instruments (Trenton, NJ) liquid N_2-cooled (LN-1100PB) charge-coupled device detector with 4 cm^{-1} spectral resolution. The 632.8-nm laser excitation line at 50 mW power was obtained with a Spectra-Physics 2030-15 argon ion laser and a 37B CW dye (Rhodamine 6G). The Raman spectra were obtained at room temperature by 90° scattering in a spinning cell, and the Raman frequencies were referenced to indene. For each sample, the entire spectral range was obtained by collecting spectra at two different frequency windows, and the resulting spectra were spliced together. Baseline corrections (polynomial fits) and curve fits (Gaussian functions) were carried out by using GRAMS/32 SPECTRAL NOTEBOOK version 4.04 (Thermo Galactic, Salem, NH).

Results

Chromophore Generated by Reaction of Succinate-Fe(II)TauD with O_2. Incubation of αKG-Fe(II)TauD with O_2 in the absence of taurine was previously found to give rise to a greenish-brown chromophore (λ_{max} 550 nm, ε_{550} 700 $M^{-1}\cdot cm^{-1}$) (Fig. 2, dot-dash line; ref. 28). On standing for several days, the color converted to bright green (λ_{max} 720 nm, ε_{720} ≈300 $M^{-1}\cdot cm^{-1}$). This new species can be accessed directly by a 2-h incubation of taurine-αKG-Fe(II)TauD with oxygen (Fig. 2, dotted trace). Because TauD rapidly catalyzes the oxidative decarboxylation of αKG to form succinate under these turnover conditions, the influence of succinate on chromophore formation was examined. Oxygen exposure of succinate-Fe(II)TauD (Fig. 2, dashed line) or taurine-succinate-Fe(II)TauD (data not shown) generated the same 720-nm feature at greater intensity (ε_{720} 380 $M^{-1}\cdot cm^{-1}$), whereas no absorption beyond 450 nm was observed for O_2-treated Fe(II)TauD (solid line) or taurine-Fe(II)TauD (dot-dot-dash trace). The reaction was specific for succinate as shown by the lack of chromophore formation by using glutarate as an alternative dicarboxylate. Additional studies were carried out to define the relationship between the 720-nm succinate-dependent chromophore and the previously reported 550-nm αKG-dependent chromophore.

Reactivity of TauD Samples with H_2O_2. To facilitate further characterization of the 720-nm TauD species, alternative oxidants were examined to speed up chromophore formation. Spectra

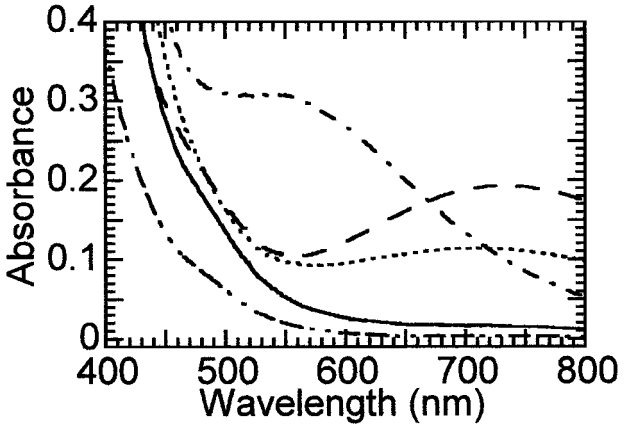

Fig. 2. Effect of O_2 on the absorption spectra of selected Fe(II)TauD states. Anaerobically prepared Fe(II)TauD samples were incubated with 100% oxygen in the headspace for at least 2 h and spectroscopically characterized. The samples included O_2-treated Fe(II)TauD (solid trace; 0.6 mM TauD subunit, 0.5 mM ferrous ammonium sulfate, and 25 mM Tris buffer, pH 8.0) and similarly treated enzyme with 3 mM taurine (dot-dot-dash line), 3 mM αKG plus 3 mM taurine (dotted line), or 3 mM succinate (dashed line). For comparison, the spectrum is shown (dot-dash line) for a sample of αKG-Fe(II)TauD mixed with an equal volume of 100% oxygen-saturated buffer after a 2-h incubation. This spectrum is adjusted in intensity so that the final enzyme and metal concentrations are equivalent to the other samples.

generated on addition of H_2O_2 to anaerobic solutions of succinate-Fe(II)TauD (Fig. 3, dashed line) and taurine-succinate-Fe(II)TauD (data not shown) closely resembled the 720-nm chromophore formed with oxygen. In contrast, no significant absorption beyond 430 nm was observed for Fe(II)TauD or taurine-Fe(II)TauD after hydrogen peroxide treatment (data not shown). Due to the rapid H_2O_2-dependent decomposition of free αKG, analogous experiments could not be carried out with this substrate. Titration experiments demonstrated that maximal formation of the ≈700-nm chromophore required ≈1.5 equivalents of hydrogen peroxide per metal ion. Significantly, the peroxide-dependent spectroscopic transformations were complete by 10 min rather than the much longer time periods required for the oxygen-dependent spectroscopic changes. The rapid changes in spectral properties of TauD

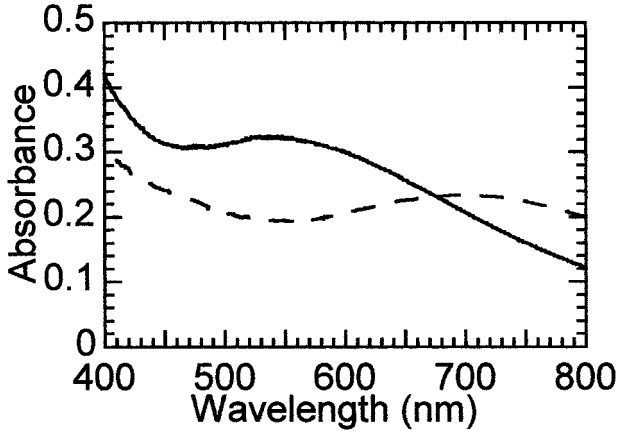

Fig. 3. Effect of H_2O_2 addition on the absorption spectra of selected Fe(II)TauD states. Anaerobically prepared succinate-Fe(II)TauD (0.6 mM TauD subunit, 0.5 mM ferrous ammonium sulfate, 3 mM succinate, and 25 mM Tris buffer, pH 8.0) was adjusted to 1.5 mM H_2O_2 and allowed to react for 20 min (dashed line). An analogous sample was prepared with the additional presence of 100 mM bicarbonate (solid trace).

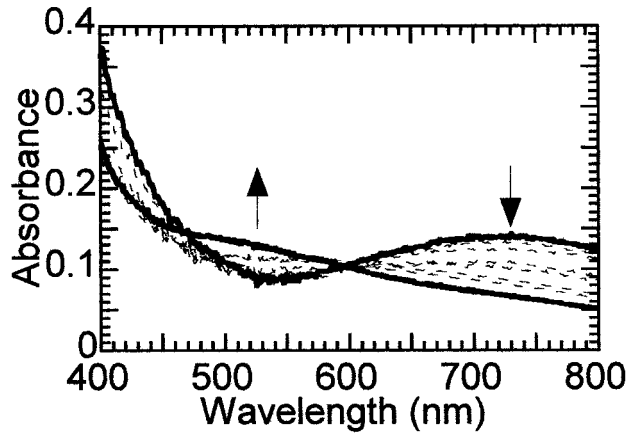

Fig. 4. Interconversion of Fe(III)-catecholate chromophores. Succinate-Fe(II)TauD was mixed with 100% O_2-saturated buffer (so the final enzyme concentration is half that shown in Fig. 2) and allowed to react for 3 h (dark solid trace). The sample was adjusted to 100 mM bicarbonate and monitored (gray traces) up to 14 h (dashed line).

samples during hydrogen peroxide-dependent oxidation were exploited to examine the reasons for the differences in the two chromophores.

Bicarbonate-Dependent Spectroscopic Interconversions. Oxidative decomposition of αKG yields both succinate and bicarbonate/CO_2; thus, the effects of bicarbonate on the spectral transformations were examined. Hydrogen peroxide-dependent oxidation of succinate-Fe(II)TauD in the presence of 100 mM bicarbonate was shown to yield a 550-nm chromophore (Fig. 3, solid line) similar to that associated with O_2-dependent oxidation of αKG-Fe(II)TauD. The presence of bicarbonate during oxygen exposure of succinate-Fe(II)TauD also affected the spectrum, resulting in what seemed to be a mixture of the 720- and 550-nm species (data not shown). When bicarbonate was added to the oxygen-exposed succinate-Fe(II)TauD sample containing the 720-nm chromophore, it promoted a slow conversion to the 550-nm chromophore (Fig. 4). Furthermore, the 550-nm chromophore obtained by hydrogen peroxide treatment of bicarbonate-succinate-Fe(II)TauD rapidly converted to the ≈700-nm chromophore in the presence of taurine (data not shown). These results are consistent with bicarbonate participating in the formation of the 550-nm chromophore, with release of this group on taurine addition to yield the bicarbonate-free ≈700-nm chromophore. The effects detailed above were specific to bicarbonate, as formate failed to elicit any of the changes observed.

Resonance Raman Characterization of the ≈700-nm Chromophore. The 550-nm chromophore was previously assigned by resonance Raman spectroscopy as arising from an Fe(III)-catecholate ligand-to-metal charge-transfer transition (28); hence, the same technique was used to further characterize the ≈700-nm species. The resonance Raman spectrum of the chromophore formed by H_2O_2 treatment of succinate-Fe(II)TauD (Fig. 5) exhibits a set of vibrations (536, 582, 644, 1,259, 1,314, 1,344, 1,424, and 1,476 cm^{-1}) that are remarkably similar to that observed for the 550-nm chromophore (544, 580, 623, 644, 1,128, 1,261, 1,314, 1,345, 1,425, and 1,475 cm^{-1}) arising from O_2 oxidation of αKG-Fe(II)TauD. The 1261 cm^{-1} band is associated with an aromatic ring deformation involving the catecholate C—O bonds (34). In the reaction of O_2 with αKG-Fe(II)TauD, the band exhibits no change when using $^{18}O_2$ in $H_2{}^{16}O$ buffer but downshifts 7

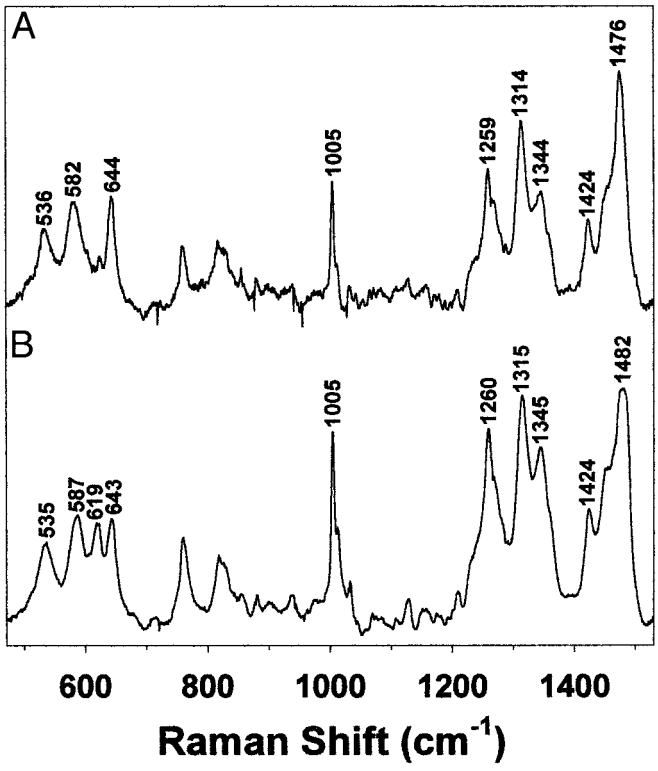

Fig. 5. Resonance Raman spectra (λ_{ex} 632.8 nm) of (*A*) the ≈700-nm species generated by H_2O_2 treatment of succinate-Fe(II)TauD (2.5 mM subunit) and (*B*) the 550-nm species generated by the addition of 100 equivalents of bicarbonate to *A*.

cm^{-1} when generated with $^{16}O_2$ in $H_2{}^{18}O$, consistent with oxygen incorporation from solvent into the newly formed catecholate of TauD (28). In addition, prior studies of the 550-nm chromophore assigned both the 623 cm^{-1} and 644 cm^{-1} features to the Fe-O4 vibration and the 580 cm^{-1} feature to the Fe-O3 stretch (28). For the H_2O_2-treated succinate-Fe(II)TauD sample, the 623 cm^{-1} feature associated with the Fe-O4 vibration either disappeared or greatly decreased in intensity, and other small shifts were observed throughout the spectrum. Furthermore, addition of 100 equivalents of bicarbonate to the sample containing the ≈700-nm species led to a splitting of the 644 cm^{-1} vibration to form a 619 cm^{-1} feature, in very close agreement to that associated with the 550-nm chromophore. Thus, both the resonance Raman and visible spectra seem sensitive to the presence of bicarbonate.

UV-Visible Spectroscopic Analysis of TauD Mutants. The similarities between the resonance Raman spectra of the ≈700-nm and 550-nm species and the ability to interconvert the two chromophores are consistent with a single catecholate species. To directly test whether the same hydroxylated Tyr residue exists in both protein forms, a site-directed mutagenesis approach was used. TauD variants with substitutions at Tyr-73 and Tyr-256 [located 6.5 and 9.3 Å from the metallocenter, respectively (26)] were previously generated and shown to retain catalytic activity (28). The apoproteins were incubated with Fe(II) plus succinate and reacted with oxygen (Fig. 6) or H_2O_2 (data not shown). The green catechol-associated absorption was formed by using Y256I, Y256F, and wild-type TauD samples (dashed, dotted, and dot-dash traces, respectively) but not with the Y73I or Y73S variants (dot-dot-dash and solid traces). These results suggest that Tyr-73 is converted to a catechol in both the 720-nm and 550-nm chromophores.

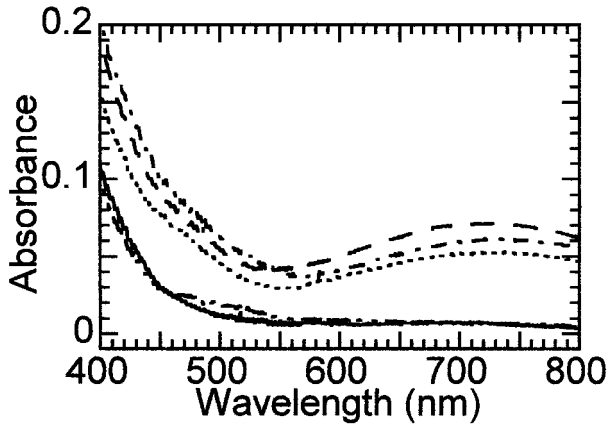

Fig. 6. UV/visible spectroscopic analysis of the reaction of succinate-bound TauD variants with oxygen. Spectra were obtained 2 h after mixing anaerobic succinate-Fe(II)TauD samples (3 mM succinate, 0.6 mM subunit, 0.5 mM ferrous ammonium sulfate in 25 mM Tris buffer, pH 8.0) with equal volumes of 100% O_2-saturated buffer (so the final enzyme concentrations are half those shown in Fig. 2). Spectra are presented for wild-type TauD (dot-dash trace) and the Y256I (dashed line), Y256F (dotted line), Y73I (dot-dot-dash), and Y73S (solid line) variants.

Discussion

Oxygen exposure of succinate-Fe(II)TauD generates an Fe(III)-catecholate chromophore at 720 nm involving Tyr-73; similar spectra are obtained by using hydrogen peroxide as an alternative oxidant, but on a much faster time scale. The intensity of this species is somewhat variable, likely reflecting the extent of tyrosine hydroxylation in each experiment. This chromophore is closely related to the 550-nm Fe(III)-catecholate species, also involving Tyr-73, formed during oxygen exposure of αKG-Fe(II)TauD (28). Significant reorganization of the active site must occur during formation of these Fe(III)-catecholate chromophores because Tyr-73 is located 6.5 Å from the metal ion in the native enzyme (26). The 550-nm chromophore converts very slowly to the 720-nm species on standing or much more rapidly on the addition of taurine, whereas the 720-nm species can be transformed into the 550-nm species by treatment with excess bicarbonate. These observations suggest the presence of an equilibrium that affects the Lewis acidity of the Fe(III) center (35).

The spectral shift between the 720-nm and 550-nm chromophores can be understood in terms of the nature of the sixth ligand bound to the metal ion, assuming that both spectroscopic species arise from Fe(III) centers coordinated by two catecholate oxygens and the aspartyl and two histidinyl side chain ligands (26). We propose that a water molecule likely occupies the sixth coordination site in the 720-nm chromophore, whereas bicarbonate (and not CO_2) fills this site in the 550-nm chromophore (Scheme 2). The replacement of a neutral ligand with the anionic bicarbonate ligand reduces the Lewis acidity of the metal center and elicits the observed blue shift in the catecholate chromophore [as well as the downshift of the Fe-O4 (dihydroxyphenylalanine) vibration in the resonance Raman spectrum]. In agreement with this explanation, catecholate complexes of other 2-His-1-carboxylate enzymes, such as phenylalanine hydroxylase and tyrosine hydroxylase, exhibit absorption maxima near 700 nm (34–36), whereas synthetic iron-catecholate complexes experience blue shifts in their ligand-to-metal charge-transfer bands as neutral ligands

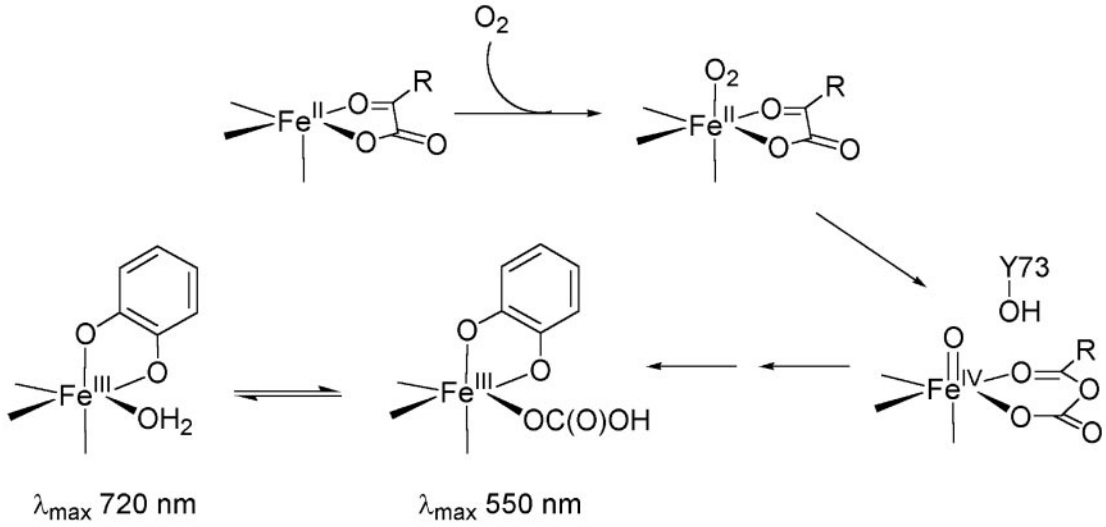

Scheme 2.

are replaced by carboxylates (35). Thus, the fact that the catecholate chromophore observed initially in the reaction of αKG-Fe(II)TauD with O_2 has an absorbance maximum at 550 nm and a resonance Raman spectrum similar to that derived from succinate-Fe(II)TauD + H_2O_2 + bicarbonate suggests that an anion becomes bound at the sixth ligand position subsequent to oxidative decarboxylation of αKG and hydroxylation of Tyr-73. We propose that this anion is the bicarbonate derived from αKG oxidation, which dissociates slowly from the active site in the absence of taurine (Scheme 2).

In contrast to the evidence presented that the αKG-derived bicarbonate anion can bind tightly to the TauD metallocenter, a crystallographic study of deacetoxycephalosporin C synthase (DAOCS) has shown nonhydrated CO_2 coordinates the metal center (37). This result was obtained with a mutant DAOCS (ΔR307A) in which the five carboxyl-terminal residues (ArgThrSerLysAla) were replaced by one Ala residue, thereby allowing greater access to the active site. This variant enzyme exhibits greatly enhanced uncoupling (i.e., oxidative αKG decomposition is less tightly coupled to substrate hydroxylation). The ΔR307A DAOCS protein was crystallized in the presence of 5 mM succinate and 5 mM bicarbonate, and the 1.96-Å resolution structure revealed that unhydrated CO_2 and succinate both bind in a monodentate fashion to the metal. Significantly, the C-4 carboxylate of the organic acid is not stabilized by an interaction with Arg-258 or Ser-260 as was shown for the C-5 carboxylate of αKG in the crystal structure of the wild-type DAOCS-αKG complex (13). Thus, it is possible that the structure observed for DAOCS in the presence of succinate and bicarbonate may differ significantly from that obtained when αKG is decarboxylated at the active site. Alternatively, the redox state of the metal may account for the observed coordination differences between the enzymes, with bicarbonate binding to the oxidized metal site of TauD and CO_2 binding to the reduced iron of DAOCS.

The interaction of bicarbonate with the TauD metal site is somewhat reminiscent of results obtained with another superfamily member, 1-aminocyclopropane-1-carboxylate (ACC) oxidase. Carbon dioxide has long been known to activate ACC oxidase (38), and this activation was recently examined by a series of spectroscopic studies (39). In the absence of carbon dioxide, the six-coordinate metal site becomes five coordinate when the substrate ACC binds, thus creating a site for oxygen reactivity. However, this form of ACC oxidase is rapidly inactivated by dioxygen in the absence of the cosubstrate ascorbate, presumably due to side chain hydroxylations analogous to the reactions described here for TauD as well as cleavage of the peptide backbone (40). Conversely, when ACC is added in the presence of carbon dioxide, the activator is proposed to react with a solvent molecule coordinated to the metal, forming a metal-bound bicarbonate at the sixth coordination site, which blocks dioxygen binding and therefore protects the enzyme from self-hydroxylation or other inactivating reactions. Addition of ascorbate leads to the displacement of bicarbonate and ultimately product formation. Further studies are required to assess whether the protective effect of metal-bound bicarbonate found with ACC oxidase may apply more generally to the αKG-dependent dioxygenase family. Nevertheless, the results reported in this paper provide clear evidence for bicarbonate binding to the metal center in TauD during the course of oxygen activation.

This work was supported by National Institutes of Health Grants GM063584 (to R.P.H.) and GM33162 (to L.Q.). K.D.K. acknowledges support from National Institutes of Health Chemistry Biology Interface Training Grant GM-08700.

1. Eichhorn, E., van der Ploeg, J. R., Kertesz, M. A. & Leisinger, T. (1997) *J. Biol. Chem.* **272,** 23031–23036.
2. Prescott, A. G. & Lloyd, M. D. (2000) *Nat. Prod. Rep.* **17,** 367–383.
3. Ryle, M. J. & Hausinger, R. P. (2002) *Curr. Opin. Chem. Biol.* **6,** 193–201.
4. Solomon, E. I., Brunold, T. C., Davis, M. I., Kemsley, J. N., Lee, S.-K., Lehnert, N., Neese, F., Skulan, A. J., Yang, Y.-S. & Zhou, J. (2000) *Chem. Rev.* **100,** 235–349.
5. Kivirikko, K. I. & Pihlajaniemi, T. (1998) *Adv. Enzymol. Rel. Areas Mol. Biol.* **72,** 325–398.
6. Hewitson, K. S., McNeill, L. A., Riordan, M. V., Tian, Y.-M., Bullock, A. N., Welford, R. W., Elkins, J. M., Oldham, N. J., Bhattacharya, S., Gleadle, J. M., *et al*. (2002) *J. Biol. Chem.* **277,** 26351–26355.
7. Trewick, S. C., Henshaw, T. F., Hausinger, R. P., Lindahl, T. & Sedgwick, B. (2002) *Nature* **419,** 174–178.
8. Fukumori, F. & Hausinger, R. P. (1993) *J. Biol. Chem.* **268,** 24311–24317.
9. Hogan, D. A., Auchtung, T. A. & Hausinger, R. P. (1999) *J. Bacteriol.* **181,** 5876–5879.
10. Kahnert, A. & Kertesz, M. A. (2000) *J. Biol. Chem.* **275,** 31661–31667.
11. Thornburg, L. D. & Stubbe, J. (1993) *Biochemistry* **32,** 14034–14042.
12. Roach, P. L., Clifton, I. J., Fülöp, V., Harlos, K., Barton, G. J., Hajdu, J., Andersson, K., Schofield, C. J. & Baldwin, J. E. (1995) *Nature* **375,** 700–704.
13. Valegård, K., Terwisscha van Scheltinga, A. C., Lloyd, M. D., Hara, T.,

Ramaswamy, S., Perrakis, A., Thompson, A., Lee, W.-J., Baldwin, J. E., Schofield, C. J., *et al*. (1998) *Nature* **394,** 805–809.
14. Zhang, Z., Ren, J., Stammers, D. K., Baldwin, J. E., Harlos, K. & Schofield, C. J. (2000) *Nat. Struct. Biol.* **7,** 127–133.
15. Wilmouth, R. C., Turnbull, J. J., Welford, R. W. D., Clifton, I. J., Prescott, A. G. & Schofield, C. J. (2002) *Structure* **10,** 93–103.
16. Hedden, P. (1999) *J. Exp. Bot.* **50,** 553–563.
17. Mukherji, M., Chien, W., Kershaw, N. J., Clifton, I. J., Schofield, C. J., Wierzbicki, A. S. & Lloyd, M. D. (2001) *Hum. Mol. Genet.* **10,** 1971–1982.
18. Vaz, F. M., Ofman, R., Westinga, K., Back, J. W. & Wanders, R. J. A. (2001) *J. Biol. Chem.* **276,** 33512–33517.
19. Schofield, C. J. & Zhang, Z. (1999) *Curr. Opin. Struct. Biol.* **9,** 722–731.
20. Saari, R. E. & Hausinger, R. P. (1998) *Biochemistry* **37,** 3035–3042.
21. Ryle, M. J., Padmakumar, R. & Hausinger, R. P. (1999) *Biochemistry* **38,** 15278–15286.
22. Hegg, E. L., Whiting, A. K., Saari, R. E., McCracken, J., Hausinger, R. P. & Que, L., Jr. (1999) *Biochemistry* **38,** 16714–16726.
23. Hogan, D. A., Smith, S. R., Saari, E. A., McCracken, J. & Hausinger, R. P. (2000) *J. Biol. Chem.* **275,** 12400–12409.
24. Ho, R. Y. N., Mehn, M. P., Hegg, E. L., Liu, A., Ryle, M. A., Hausinger, R. P. & Que, L., Jr. (2001) *J. Am. Chem. Soc.* **123,** 5022–5029.
25. Liu, A., Ho, R. Y. N., Que, L., Jr., Ryle, M. J., Phinney, B. S. & Hausinger, R. P. (2001) *J. Am. Chem. Soc.* **123,** 5126–5127.
26. Elkins, J. M., Ryle, M. J., Clifton, I. J., Dunning Hotopp, J. C., Lloyd, J. S., Burzlaff, N. I., Baldwin, J. E., Hausinger, R. P. & Roach, P. L. (2002) *Biochemistry* **41,** 5185–5192.
27. Dunning Hotopp, J. C. & Hausinger, R. P. (2002) *Biochemistry* **41,** 9787–9794.
28. Ryle, M. J., Liu, A., Muthukumaran, R. B., Ho, R. Y. N., Koehntop, K. D., McCracken, J., Que, L., Jr., & Hausinger, R. P. (2003) *Biochemistry* **42,** 1854–1862.
29. Hegg, E. R., Ho, R. Y. N. & Que, L., Jr. (1999) *J. Am. Chem. Soc.* **121,** 1972–1973.
30. Logan, D. T., deMaré, F., Persson, B. O., Slaby, A., Sjöberg, B.-M. & Nordlund, P. (1998) *Biochemistry* **37,** 10798–10807.
31. Baldwin, J., Voegtli, W. C., Khidekel, N., Moënne-Loccoz, P., Krebs, C., Pereira, A. S., Ley, B. A., Huynh, B. H., Loehr, T. M., Riggs-Gelasco, P. J., *et al*. (2001) *J. Am. Chem. Soc.* **123,** 7017–7030.
32. Bradley, F. C., Lindstedt, S., Lipscomb, J. D., Que, L., Jr., Roe, A. L. & Rundgren, M. (1986) *J. Biol. Chem.* **261,** 11693–11696.
33. Serre, L., Sailland, A., Sy, D., Boudec, P., Rolland, A., Pebay-Peyroula, E. & Cohen-Addad, C. (1999) *Structure* **7,** 977–988.
34. Michaud-Soret, I., Andersson, K. K., Que, L., Jr., & Haavik, J. (1995) *Biochemistry* **34,** 5504–5510.
35. Cox, D. D., Benkovic, S. J., Bloom, L. M., Bradley, F. C., Nelson, M. J., Que, L., Jr., & Wallick, D. E. (1988) *J. Am. Chem. Soc.* **110,** 2026–2032.
36. Andersson, K. K., Cox, D. D., Que, L., Jr., Flatmark, T. & Haavik, J. (1988) *J. Biol. Chem.* **263,** 18621–18626.
37. Lee, H. J., Lloyde, M. D., Clifton, I. J., Baldwin, J. E. & Schofield, C. J. (2001) *J. Mol. Biol.* **308,** 937–948.
38. Dong, J. G., Fernàndez-Maculet, J. C. & Yang, S. F. (1992) *Proc. Natl. Acad. Sci. USA* **89,** 9789–9793.
39. Zhou, J., Kelly, W. L., Bachmann, B. O., Gunsior, M., Townsend, C. A. & Solomon, E. I. (2001) *J. Am. Chem. Soc.* **123,** 7388–7398.
40. Zhang, Z., Barlow, J. N., Baldwin, J. E. & Schofield, C. J. (1997) *Biochemistry* **36,** 15999–16007.